Materials Today: Proceedings 45 (2021) 6381–6385

Contents lists available at ScienceDirect

Materials Today: Proceedings

journal homepage: www.elsevier.com/locate/matpr

CFD analysis of viscous fingering in Hele-Shaw cell for air-glycerin system

Akhileshwar Singh *, Krishna Murari Pandey, Yogesh Singh

Department of Mechanical Engineering, National Institute of Technology Silchar, Assam 788010, India

ARTICLE INFO

Article history:
Received 7 October 2020
Received in revised form 1 November 2020
Accepted 4 November 2020
Available online 19 December 2020

Keywords:
Numerical analysis
Viscous fingering
Hele-Shaw cell
Immiscible fluids
Two-phase flow
VOF model

ABSTRACT

In this research paper, a numerical study has been done on the viscous fingering instability for the air-glycerin system in the 2D horizontal Hele-Shaw cell. The air and glycerin are immiscible fluids and the viscosity of glycerin is too much higher than air and viscous fingering strongly depends upon the viscosity differences of fluids pairs so that the air-glycerin system is taken. In this work, an immiscible fluid–fluid displacement flow process occurs and a low viscous fluid air displaces another high viscous fluid glycerin in the rectangular Hele-Shaw cell then due to unstable displacement of glycerin by air a single finger shape instability appears at the air-glycerin interface. This phenomenon is called viscous fingering. The viscous fingering has got importance in many natural and industrial applications such as geologic carbon dioxide sequestration, oil recovery, water infiltration into the soil, mixing of fluids at low Reynolds numbers in microfluidic devices, and many more. This numerical simulation is based on the transient solver. Volume of fluid (VOF) model has been accounted for tracking of the air- glycerin interface. The Geo-reconstruct scheme has been selected for precise interface tracking. The PISO (Pressure Implicit with Splitting of Operators) scheme has been adopted because it has improved the calculation efficiency. The objectives of this paper are to track the growth of a single finger at the air-glycerin interface and calculate the displacement efficiency by image processing. We found that air displaces only 74.15% of glycerin from the entire cell. We have also shown the distribution of pressure and velocity in the entire cell domain.
© 2020 Elsevier Ltd. All rights reserved.
Selection and peer-review under responsibility of the scientific committee of the International Conference on Mechanical, Electronics and Computer Engineering 2020: Materials Science.

1. Introduction

Saffman and Taylor [1] had been introduced the viscous fingering in 1958. They observed that whenever a high viscous fluid is driven by another low viscous fluid in a porous medium or Hele-Shaw cell (one pair of flat glass plates separated by a narrow gap), then channel or finger-like pattern forms at the fluid–fluid interface due to unstable displacement flow. This phenomena is called viscous fingering or Saffman-Taylor instability. The viscous fingering has got importance in many natural and industrial applications such as carbon dioxide sequestration [2], secondary and tertiary oil recovery [3], water infiltration into the soil, mixing of fluids in microfluidic devices [4], lung biomechanics [5] and so on. Viscous fingering is undesirable in enhance oil recovery because it decreases the sweep efficiency [6] so that the efficiency of enhance oil recovery decreases. Further, dendritic formation in the lithium-ion batteries due to viscous fingering and dendritic is responsible for internal short circuits and accidents in batteries [7]. The viscous fingering increases the mixing efficiency in microfluidic devices by creating disorder in the velocity field [8]. The viscous fingering increases the CO2 mixing in saline aquifers for carbon sequestration [9]. From the above applications, it can be concluded that viscous fingering has both merits and demerits according to its applications. Therefore, active control (suppress or promote) of the viscous fingering is fascinating in industrial applications.

A. Singh et al. [10,11] wrote reviews on viscous fingering pattern formation in radial and lifted Hele-Shaw cells and explored the effect of operating parameters (e.g., injection rate, viscosity ratio, the gap between plates, and many more) on the viscous finger morphology.

The Hele-Shaw cell (HSC) apparatus is used for the study of flow in a porous medium because the flow in HSC is similar to the flow in the porous medium [12]. The viscous fingering instability has

* Corresponding author.
E-mail address: akhileshwarsinghs@gmail.com (A. Singh).

https://doi.org/10.1016/j.matpr.2020.11.069
2214-7853/© 2020 Elsevier Ltd. All rights reserved.
Selection and peer-review under responsibility of the scientific committee of the International Conference on Mechanical, Electronics and Computer Engineering 2020: Materials Science.

been widely studied for Newtonian and non-Newtonian fluids displaced by air in the HSC [13–19]. The researchers have been commonly used air as a displacing fluid in fluid–fluid displacement flow processes because it is offered large viscosities differences and densities differences between the fluids. The viscous fingering is seen in both miscible and immiscible fluids displacement flow [20–24]. Varges et al. [24] studies the immiscible fluids displacement flow in HSC and observed that the stability of the interface strongly depends on the viscosity ratio. They also observed that large numbers of branches were developed at the low viscosity ratio. Nittmann [25] reported that the single finger can be broken into two equal fingers by increasing the capillary number (ratio of viscous force and capillary force) with the help of increasing the flow rate. It means that capillary forces are played an important role to damp the splitting of the fingertip.

In the fluids displacement flow processes in the porous medium, the following forces are involved [26]: viscous forces driven by adverse viscosity ratios, gravity forces due to density differences, capillary forces due to interfacial tension between immiscible fluids, and dispersive forces due to concentration gradients between miscible fluids. These forces are responsible for an unstable displacement flow. We know that the fluids displacement flow in HSC is analogous to fluids displacement flow in homogeneous porous media and if two phases are immiscible so that the effect of dispersive forces can be neglected. If the orientation of HSC is horizontal then the effect of gravity forces can be also neglected. The present numerical study has been performed on horizontal HSC therefore viscous force and capillary force are acting. But we are selected a low capillary number ($Ca < 1$) to neglect the effect of capillary force and to damp finger splitting. Therefore, the viscous force is the only cause of unstable displacement flow in this study.

This research has three objectives: (I) to simulate the unstable immiscible fluids displacement flows in a rectangular HSC including surface tension effects and to develop single finger at fluids interface, (II) to capture the growth of single finger and calculate the displacement efficiency by image processing, and (III) to show the velocity and pressure distribution in entire HSC. The viscous fingering pattern formation for the air-glycerin system has been done numerically. The governing equations have been solved by ANSYS fluent tool.

2. Geometry modeling and grid generation

The geometry of 2D rectangular Hele-Shaw cell (HSC) with proper boundaries and image of the meshed computational domain is shown in Fig. 1 and Fig. 2 respectively. The geometry and meshed computational domain have been created by ANSYS FLUENT drawing and meshing modules. The length (L) and width (w) of rectangular HSC have been taken 10 cm and 2 cm respectively. The fine square structural grids have been created by the mapped mesh method.

We carried out the grid-independent test and found that the shape of the interface was not depending on grid size when the number of elements in the meshed computational domain was more than 117000. Therefore, we considered the number of elements in the computational domain 188000.

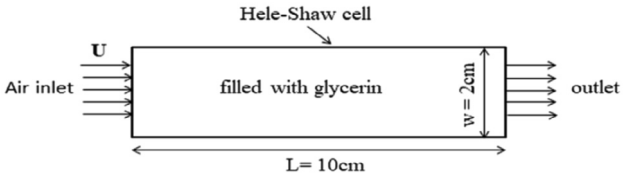

Fig. 1. Top view of horizontal Hele-Shaw cell.

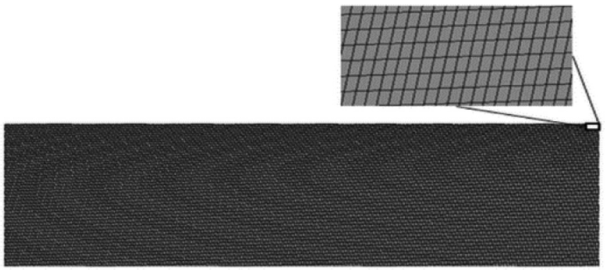

Fig. 2. Meshed computational domain.

3. Mathematical and numerical modeling

The numerical simulations of viscous fingering in the 2D rectangular HSC have been performed by using the ANSYS fluent computational fluid dynamic (CFD) software [27]. This software is discretized all the equations by the control volume method. We were performed numerical experiments by considering transient flow, immiscible fluid pair, and constant fluid properties. Simulations were carried out by using a pressure-based solver and transient model. The Volume of Fluid (VOF) method has been adopted to capture the volume fraction of each fluid in the entire computational domain because it is the best choice to calculate the volume fraction of each fluid in our immiscible two-phase flow. In this method, a single set of momentum equations is shared between both the fluids.

The fluid–fluid interface is tracked by solving the volume fraction equation of each phase in the entire domain. The Geo-reconstruct scheme has been accounted for precise interface tracking. The PISO (Pressure Implicit with Splitting of Operators) scheme has been selected because it is improved the calculation efficiency. The stability of the numerical solution has been defined by considering relaxation factors less than unity and Courant number 0.5.

The displaced fluid (e.g., glycerin) and displacing fluid (e.g., air) are defined as the primary phase and secondary phase respectively. Initially, the entire domain was filled with glycerin by considering volume fraction of glycerin and air were one and zero respectively. The effect of interfacial tension along the interface had been considered and it had been taken constant throughout the study. The interfacial tension is calculated to pressure jump at the interface. The air was injected with a velocity of 0.02 through the inlet edge into the computational domain by considering the volume fraction of air and glycerin were one and zero. The air- glycerin interface was traced in the entire domain by calculating the volume fraction of each fluid in each cell of the computational domain.

3.1. Governing equations

These governing equations were solved by ANSYS FLUENT software in this numerical study.

Continuity equation:

$$\frac{\partial \rho}{\partial t} + \nabla \cdot (\rho U) = 0 \tag{1}$$

Momentum equation:

$$\frac{\partial}{\partial t}(\rho U) + \nabla \cdot (\rho UU) = -\nabla P + \nabla \cdot \mu(\nabla U + \nabla U^T) + \rho g + F_s \tag{2}$$

Surface tension force (F_s) is considered as a volumetric force in the CSF model.

$$F_s = \gamma k \nabla(\alpha) \tag{3}$$

Volume Fraction equation:

$$\frac{\partial \alpha}{\partial t} + \nabla \cdot (\alpha U) = 0 \quad (4)$$

Properties formula for two-phase flow:

$$\rho = \alpha_2 \rho_2 + (1 - \alpha_2)\rho_1 \quad (5)$$

$$\mu = \alpha_2 \mu_2 + (1 - \alpha_2)\mu_1 \quad (6)$$

The sum of volume fractions of each phase is always unity in multiphase.

$$\alpha_1 + \alpha_2 = 1 \quad (7)$$

Where, U, P, and g are denoted velocity field vector, pressure field vector, and gravity vector, respectively. ρ, μ, α ,γ, and k are denoted density, viscosity, volume fraction, interfacial tension, and curvature of the interface respectively. F_s is denoted surface tension force in the continuum surface force (CSF) model and surface tension is considered as a volumetric force in this CFD model.

The properties (density, viscosity), which are involved in Eq. (2) are calculated by Eq.5 and Eq.6. The Eq.5 and Eq.6 are represented fluid properties (density, viscosity) into the dispersed two-phase system. The subscripts 1 and 2 are denoted primary and secondary phases of fluids.

3.2. Materials properties

The air and glycerin have been selected as working fluids from ANSYS fluent database. These fluids are immiscible. The high viscous fluid, glycerin, and low viscous fluid, air are considered as primary and secondary phases respectively. The properties of these fluids are given in Table 1.

3.3. Boundary conditions

The results of numerical simulations strongly depend on the type of initial boundary conditions. In these numerical simulations, velocity inlet, pressure outlet, and stationary wall with no-slip were considered as the initial boundary conditions. Initially, the entire computational domain was filled with the primary phase by patching the value of volume fractions of primary and secondary phases were one and zero. The secondary phase was invaded through the inlet edge with a velocity of 0.02 m/s and pressure 5 kPa by considering volume fraction of the secondary phase was one in velocity inlet boundary. The outlet pressure was considered equal to the ambient pressure. All variables of boundary conditions are defined in Table 2 and NA is presented not applicable.

4. Results and discussion

In this work, viscous fingering on the interface of immiscible fluids in a rectangular HSC has been numerically analyzed using the VOF model. In this research, we have neglected the effect of inertia force, gravity force, and capillary force by considering low Reynolds numbers (Re < 1), horizontal rectangular HSC, and low capillary number (Ca < 1) respectively. Only the effect of viscous force was considered in these numerical simulations. This study aims to show numerically the propagations of finger shape instability on the interface of immiscible fluids in the fluid–fluid displacement flow process. Viscous fingering or finger shape instability appears on the interface of fluids naturally only when the viscosity ratio of fluids is less than unity (VR < 1). The viscosity ratio (VR) is defined as the ratio of the viscosity of displacing fluid and viscosity of the displaced fluid. Here viscosity contrast was the main cause of fingering instability.

Table 1
Materials properties.

Fluids	Viscosity (mPa-s)	Density (kg/ m^3)	Surface tension (N/m)
Air	0.01789	1.225	0.068
Glycerin	799	1259.9	

Table 2
Values of boundary conditions.

Boundary conditions	Velocity	Pressure	Volume fraction
Velocity inlet (Air)	0.02 m/s	5 kPa	1
Pressure outlet	NA	0	NA

Initially, the entire computational domain was filled with glycerin (red color in Fig. 4a). After that air was injected into the HSC with a velocity of 0.02 m/s. In this fluid–fluid displacement flow process, the air was displacing fluid, and glycerin was displaced fluid. Air had less viscosity and high mobility but glycerin had high viscosity and low mobility. Therefore, injected air (blue color in Fig. 3.) was penetrated into the glycerin and mobilized it from the middle portion of the HSC. Because glycerin was provided less resistance near the middle portion of the cell and high resistance provided near walls. Unstable displacement flow was occurred due to unfavorable viscosity ratio and a finger shape instability (shape of blue color in Fig. 3) was formed at the interface of the air-glycerin system near the middle portion of HSC. It is called viscous fingering phenomena. This phenomenon occurs in a very fast manner. Therefore tracking of the interface (air-glycerin) is a big challenge. The transit VOF model with the geo-reconstruct scheme has been assigned for precise interface tracking. The red color represents the volume fraction of glycerin and the blue color represents the volume fraction of air in the computational domain.

The counters of glycerin volume fraction at various time steps are predicted the growth of finger in HSC. The growth of the finger at various time steps is shown in Fig. 4. The time steps are taken in second (s). Fig. 4a. is represented the initial condition when glycerin is kept stationary in the computational domain. After that air is injected into the domain and it is mobilized the stationary glycerin. Initially, stable displacement occurred after that unstable displacement. Due to unstable displacement of glycerin by air in HSC, the symmetrical finger shape instability (blue color) forms around the longitudinal axis of the cell. We captured the propagation of the finger at air-glycerin interface and shown in Fig. 4.

We have used the image J software for analysis of the final volume fraction image and found that approximate 74.15% of glycerin is displaced by air in the cell but 25.85% of glycerin remains in the cell. It is called residual glycerin. The air and glycerin are shown by white and black colors in Fig. 5. Using the shape of the interface of the final image, we define the displacement efficiency (η_d) as:

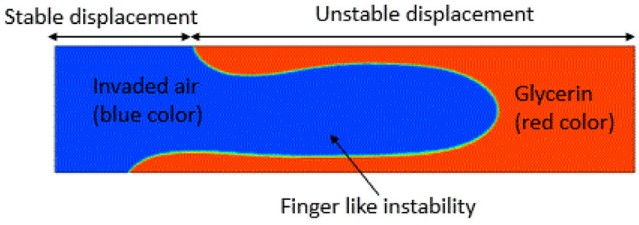

Fig. 3. Counter of finger-like instability formation or viscous fingering at air-glycerin interface.

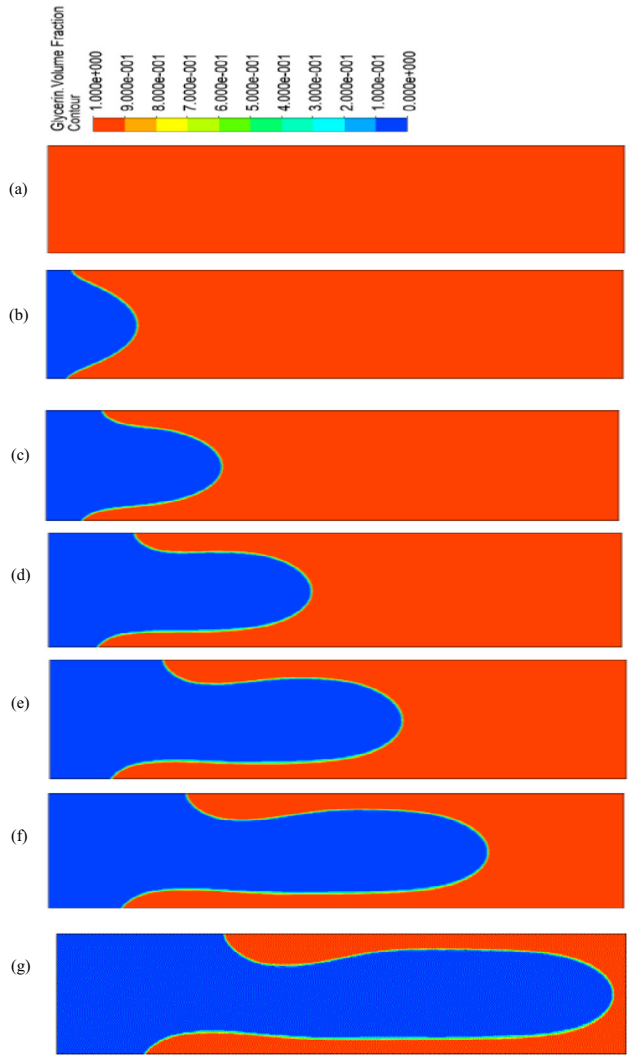

Fig. 4. Counters of glycerin volume fraction at various times (a) t = 0 s (b) t = 0.45 s (c) t = 0.90 s (d) t = 1.35 s (e) t = 1.80 s (f) t = 2.25 s (g) t = 2.70 s.

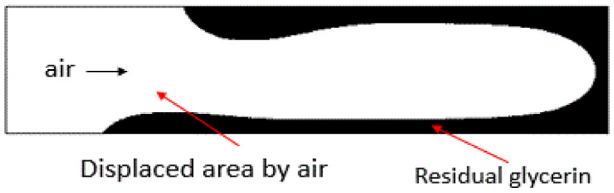

Fig. 5. Represented approximately 74.15% glycerin displaced by air in the cell.

$$\eta_d = \frac{A_d}{A_t}$$

Where, A_d is denoted area of the displaced fluid in the HSC (white pixels) and A_t is the total area $(L \times W)$ of the HSC.

The velocity counter is shown in Fig. 6. It is represented the velocity distribution of air inside the entire HSC. The red zone in the velocity counter is denoted maximum velocity field in HSC and the blue zone is denoted minimum velocity field in the HSC. The velocity is maximum near the middle portion of the cell because glycerin is offered less resistance at that location and the velocity is approximately zero near the walls because near the walls glycerin is offered higher resistance.

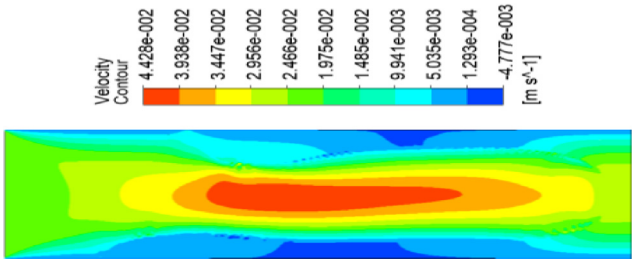

Fig. 6. Counter of the velocity profile.

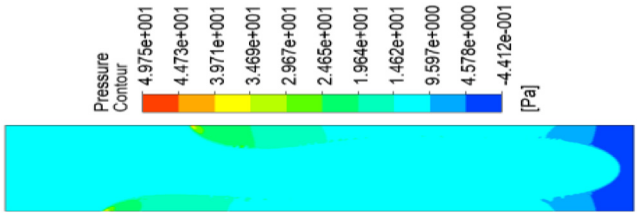

Fig. 7. Counter of the pressure profile.

The pressure counter is shown in Fig. 7. It is represented pressure distribution inside the cell. The pressure drop is maximum near the walls and minimum near the middle portion of HSC because of the high resisting force offered by glycerin near the walls so that pressure drop is maximum at that location.

5. Conclusions

In this research paper, we present the computational results of a numerical study of an immiscible fluid–fluid displacement flows in a rectangular HSC including surface tension effects. The fluid–fluid displacement flow always forms an unstable interface when the low viscous fluid displaces a high viscous fluid. It is called unstable displacement flow and this phenomena is called viscous fingering. In this numerical analysis, a high viscous glycerine was displaced by low viscous air in rectangular HSC and due to unstable displacement flow, a finger shape instabilities has appeared at the air-glycerine interface. This instability was continually growing in the direction of fluid displacement. The propagation of a single finger at the air-glycerine interface at various times are shown in Fig. 4. From these figures, we can conclude that the displacement efficiency decreases due to viscous fingering.

We found that by image processing of the final image (Fig. 4g), only 74.15% of glycerin was displaced by air from the HSC cell and the remaining 25.85% of glycerin was present in the cell due to viscous fingering. Otherwise, in the absence of viscous fingering displacement efficiency might be 100%. Present work shows that the exiting findings by numerical simulations whenever less viscous fluid displaces another high viscous fluid then finger-like instability always appears at the fluid–fluid interface. This instability always decreases the displacement efficiency or sweep efficiency. The displacement efficiency can be improved by suppressing the viscous fingering.

Similar types of interfacial instabilities are seen in oil recovery, carbon dioxide sequestration and many more natural and industrial applications so that this work will provide a time-saving and economical approach to perform numerical experiments in the fields of unstable displacement flow processes.

Author contributions

A. Singh performed numerical simulation. K.M. Pandey and Y. Singh suggested this work and drafted the manuscript.

Declaration of Competing Interest

The authors declare that they have no known competing financial interests or personal relationships that could have appeared to influence the work reported in this paper.

References

[1] P.G. Saffman, G.I. Taylor, The penetration of a fluid into a porous medium or Hele-Shaw cell containing a more viscous liquid, Proc. R. Soc. Lond. A 245 (1242) (1958) 312–329.
[2] H.E. Huppert, J.A. Neufeld, The fluid mechanics of carbon dioxide sequestration, Annu. Rev. Fluid Mech. 46 (2014) 255–272.
[3] S.B. Gorell, G.A. Homsy, Theory of the optimal policy of oil recovery by secondary displacement processes, SIAM J. Appl. Math. 43 (1983) 79–98.
[4] H.A. Stone, A.D. Stroock, A. Ajdari, Engineering flows in small devices: microfluidics toward a lab-on-a-chip, Annu. Rev. Fluid Mech. 36 (2004) 381–411.
[5] M. Heil, A.L. Hazel, Fluid-structure interaction in internal physiological flows, Annu. Rev. Fluid Mech. 43 (2011) 141–162.
[6] Z. Kargozarfard, M. Riazi, S. Ayatollahi, Viscous fingering and its effect on areal sweep efficiency during waterflooding: an experimental study, Pet. Sci. 16 (1) (2019) 105–116.
[7] P. Bai, J. Li, F.R. Brushett, M.Z. Bazant, Transition of lithium growth mechanisms in liquid electrolytes, Energy Environ. Sci. 9 (10) (2016) 3221–3229.
[8] B. Jha, L. Cueto-Felgueroso, R. Juanes, Fluid mixing from viscous fingering, Phys. Rev. Lett. 106 (19) (2011) 194502.
[9] M.R. Soltanian, M.A. Amooie, N. Gershenzon, Z. Dai, R. Ritzi, F. Xiong, D. Cole, J. Moortgat, Dissolution trapping of carbon dioxide in heterogeneous aquifers, Environ. Sci. Technol. 51 (13) (2017) 7732–7741.
[10] A. Singh, Y. Singh, K.M. Pandey, Viscous fingering instabilities in radial Hele-Shaw cell: A review, Mater. Today Proc. (2020).
[11] A. Singh, Y. Singh, K.M. Pandey, A review on viscous fingering pattern formation in lifted Hele-Shaw cell, J. Phys. Conf. Ser. 1455 (2020) 012022.
[12] G.M. Homsy, Viscous fingering in porous media, Annu. Rev. Fluid Mech. 19 (1987) 271–311.
[13] A. Lindner, D. Bonn, E.C. Poire, M. Ben Amar, J. Meunier, Viscous fingering in non-Newtonian fluids, J. Fluid Mech. 469 (2002) 237–256.
[14] L. Kondic, M.J. Shelley, P. Palffy-Muhoray, Non-Newtonian Hele-Shaw flow and the Saffman-Taylor instability, Phys. Rev. Letter 80 (1998) 1433–1436.
[15] M. Kawagushi, A. Shibata, K. Shimomoto, T. Kato, Effect of geometry and anisotropy of Hele-Shaw cell on viscous fingering of polymer solutions, Phys. Rev. E 58 (1998) 785–788.
[16] M.G. Moore, A. Juel, J.M. Burgess, W.D. McCormick, H.L. Swinney, Fluctuations in viscous fingering, Phys. Rev. E 65 (2002) 030601.
[17] T.T. Al-Housseiny, P.A. Tsai, H.A. Stone, Control of interfacial instabilities using flow geometry, Nat. Phys. 8 (10) (2012) 747–750.
[18] J.V. Fontana, E.O. Dias, J.A. Miranda, Controlling and minimizing fingering instabilities in non-Newtonian fluids, Phys. Rev. E 89 (1) (2014) 013016.
[19] A. Eslami, S.M. Taghavi, Viscous fingering regimes in elasto-visco-plastic fluids, J. Non-Newtonian Fluid Mech. 243 (2017) 79–94.
[20] J. Fernandez, P. Kurowski, P. Petitjeans, E. Meiburg, Density-driven unstable flows of miscible fluids in a Hele-Shaw cell, J. Fluid Mech. 451 (2002) 239.
[21] A. Aubertin, G. Gauthier, J. Martin, D. Salin, L. Talon, Miscible viscous fingering in microgravity, Phys. Fluids 21 (5) (2009) 054107.
[22] J.S. Nijjer, D.R. Hewitt, J.A. Neufeld, The dynamics of miscible viscous fingering from onset to shutdown, J. Fluid Mech. 837 (2018) 520–545.
[23] P.G. Saffman, Viscous fingering in Hele-Shaw cells, J. Fluid Mech. 173 (1986) 73–94.
[24] P.R. Varges, P.E. Azevedo, B.S. Fonseca, P.E. de Souza Mendes, M.F. Naccache, A. L. Martins, Immiscible liquid-liquid displacement flows in a Hele-Shaw cell including shear thinning effects, Phys. Fluids 32 (1) (2020) 013105.
[25] J. Nittmann, Fractal viscous fingering: Experiments and models, Phys. A 140 (1986) 124–133.
[26] D.E.N. Wijeratne, B.M. Halvorsen, Computational study of fingering phenomenon in heavy oil reservoir with water drive, Fuel 158 (2015) 306–314.
[27] ANSYS Fluent 12 Theory Guide book.